Incommensurate charge stripe ordering in $La_{2-x}Sr_xNiO_4$ for $x=(0.33,0.30,0.275)$

M. E. Ghazi
Physics Department, Shahrood University of Technology, Shahrood, P.O. Box 36155-316, Iran

P. D. Spencer, S. B. Wilkins, and P. D. Hatton*
Department of Physics, University of Durham, Rochester Building, South Road, Durham DH1 3LE, United Kingdom

D. Mannix
XMaS CRG, European Synchrotron Radiation Facility, 38043 Grenoble Cedex, France

D. Prabhakaran and A. T. Boothroyd
Department of Physics, University of Oxford, Clarendon Laboratory, Parks Road, Oxford OX1 3PU, United Kingdom

S.-W. Cheong
Department of Physics and Astronomy, Rutgers University, New Jersey 08854, USA
(Received 26 April 2004; published 15 October 2004)

In this paper we report studies of the charge stripe ordering using high resolution x-ray scattering in the nickelate system $La_{2-x}Sr_xNiO_4$ with doping levels of $x=0.33$, $x=0.30$, and $x=0.275$. The charge stripes for all doping levels were found to be two dimensional in nature with a high degree of correlation in the *a-b* plane. The in-plane inverse correlation length in the lower doped systems was greater than that in the $x=0.33$ system and is greatest for $x=0.275$, consistent with the stripes becoming less correlated as the doping level is decreased from $x=0.33$. However, the charge ordering in the $x=0.33$ system was observed to be more two dimensional in nature with a greater inverse correlation length between planes. The interaction between the lattice and charge order was observed to stabilize the charge ordering, even in the absence of spin ordering. In the $x=0.30$ and $x=0.275$ systems no long-range charge order could exist without the presence of the magnetic order. In both systems the charge stripes were incommensurate and on heating the incommensurability increased towards the stable $\varepsilon=0.33$ value as the stripes gained thermal energy to overcome the Coulombic repulsion. In all these systems the integrated intensity of the stripe reflections showed a clear difference in behavior from previous neutron studies with an initial increase in the integrated intensity as the temperature was increased, which was not found in the neutron studies.

DOI: 10.1103/PhysRevB.70.144507 PACS number(s): 61.10.Nz, 68.35.Rh, 71.27.+a, 71.30.+h

I. INTRODUCTION

The nickelates have attracted great interest after the discovery of a possible relationship between charge stripe ordering and high temperature superconductivity in the isostructural cuprate system.[1] $La_{2-x}Sr_xNiO_4$, which is isostructural with $La_{2-x}Sr_xCuO_4$, shows charge stripe ordering at low temperatures, and has been chosen as a candidate for the study of the relationship between charge ordering and superconductivity. The parent compounds La_2NiO_4 and La_2CuO_4 are both antiferromagnetic Mott insulators with the layered perovskite K_2NiF_4 structure. By substituting strontium for lanthanum holes are doped into the system, and this changes the properties of both systems from insulating to metallic behavior. However, the critical hole concentrations are considerably different between the two systems. The cuprate system displays weak, diffuse charge stripes, whereas the nickelate system displays strong well correlated charge stripes. In the nickelates, metallic behavior does not occur until approximately $x=1$ (Ref. 2) and at no doping level does the material display superconductivity, whereas $La_{2-x}Sr_xCuO_4$ becomes metallic and displays superconductivity for x as small as 0.05. The nickelates are a model stripe system and any understanding may be useful to explore the relationship between charge stripes and high temperature superconductivity.

The holes doped into the lattice are mobile and drastically change the properties of the $La_{2-x}Sr_xNiO_4$ system. Below the charge ordering temperature, T_{CO}, the holes segregate to form stripes and below T_N the spins order in the region between the charge stripes. The spacing between the stripes is dependant on the hole concentration n_h. The hole rich stripes act as π domain walls for the local antiferromagnetic order, existing in the hole deficient regions with nickel moments parallel to the stripe propagation direction. Such charge and spin stripes form within the *a-b* plane of the material, and are found to be two dimensional in nature. For comparison with previous data we will index the nickelate system with the $F4/mmm$ unit cell as opposed to the tetragonal $I4/mmm$ unit cell. A schematic of the charge and spin stripes in the *a-b* plane in the $F4/mmm$ setting is shown in Fig. 1. The charge and spin stripes have been confirmed in a wide variety of Sr concentrations from $x=0.135$ to 0.50,[3–6] in stark contrast with the previously accepted idea that ordering is restricted to commensurate values.[7] The wave vectors for the charge and spin stripes are $Q_{CO}=(2\varepsilon,0,1)$ and $Q_{SO}=(1\pm\varepsilon,0,0)$, respectively.

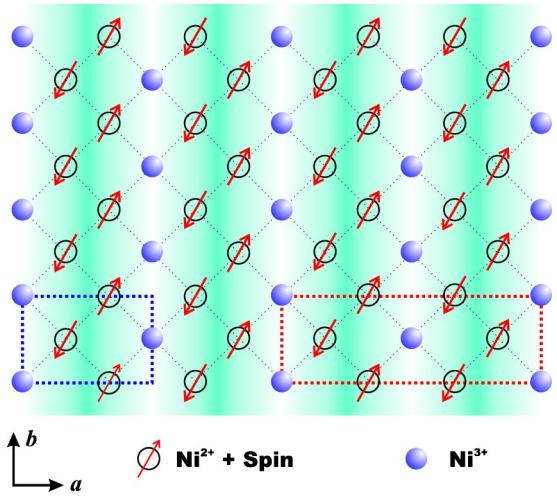

FIG. 1. (Color online) A schematic representation of the charge and spin stripes in $La_{1.67}Sr_{0.33}NiO_4$. Ni^{3+} ions are shown as filled circles and the Ni^{2+} ions are represented as open circles with the associated spin vector. The spins are believed to be canted away from the stripe direction. The dotted lines show the spin and charge supercells, respectively, and the shading shows the charge density distribution.

The $x=0.33$ composition was thought to be a special case due to the charge and spin stripes being coincident in reciprocal space. Figure 2 shows the position of the charge and spin stripes from the neutron scattering studies by Lee and Cheong[8] and is similar to Fig. 1(d) from Yoshizawa *et al.*[9] They reported charge and spin ordering temperatures of $T_{CO}=239$ K and $T_{SO}=190$ K, respectively, with the correlation lengths of the charge stripes within the plane being approximately 3 times that of the spin stripes, leading them to the conclusion that the charge correlations drive the spin ordering. More recent neutron scattering studies over the doping region $0.289<x<0.5$ (Ref. 9) have shown that the charge and spin stripe ordering temperatures maximize for $x=0.33$ and the incommensurability was found to "lock into" a value of $\varepsilon=0.33$. Away from this doping level in both directions of the stoichiometry suppression of the transition temperature is observed and the stripes become increasingly incommensurate. From this it was concluded that in the $n_h=0.33$ system, the strong electron-lattice coupling helps to stabilize the stripe ordering because of their coincidence in reciprocal space.

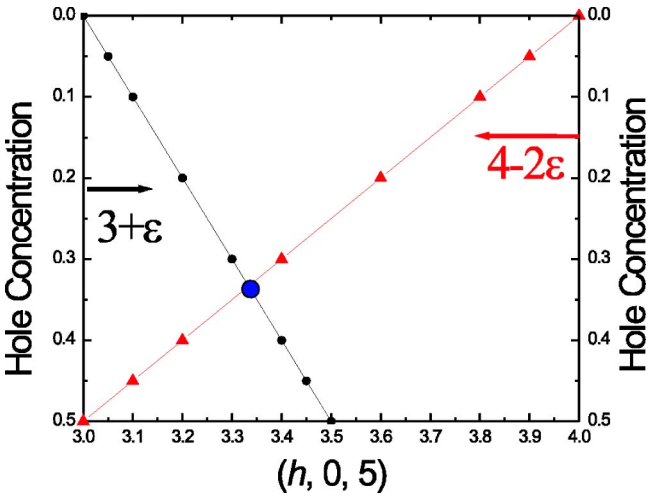

FIG. 2. (Color online) A schematic representation of how the spin (circles) and charge order (triangles) positions vary with doping. The large circle marks the doping level where the charge and spin ordering coincide at the same point in space and this corresponds to the 0.33 doping level. This is similar to Fig. 1(d) from Ref. 9.

Our previous studies on the $x=0.33$ system[10–12] using high resolution x-ray scattering have shown the stripes to be two dimensional, quenched, and disordered at low temperatures and we observed a T_{CO} of 240 K. Initially the charge ordering intensity increases when the temperature is increased from a base temperature of 10 K, which differed greatly from the previous neutron results. Also reported was the presence of critical scattering charge fluctuations above T_{CO}, which could not be observed with neutrons but could be observed with x-rays due to the high flux available from synchrotron sources.

In this paper we report on measurements of the $x=0.33$, $x=0.30$, and $x=0.275$ doped systems using high resolution x-ray scattering. These doping levels are being studied in order to gain a greater understanding of the relationship between the charge ordering and the hole doping level. Synchrotron x-rays measurements have advantages over neutron measurements due to the high flux and high wave vector resolution. In this paper we present the variation of the inverse correlation length, integrated intensity, and commensurability with temperature in each of the three samples.

II. EXPERIMENTAL DETAILS

High quality single crystal samples of $La_{2-x}Sr_xNiO_4$ with $x=0.30$ and $x=0.275$ were grown using the floating zone method at Oxford University.[13] The $x=0.33$ sample was grown at Bell laboratories. The crystal structure was found to be tetragonal with $I4/mmm$ symmetry at room temperature, but for comparison with previous work the samples were indexed with the $F4/mmm$ setting with lattice parameters $a=b\simeq 5.4145$ Å and $c=12.715$ Å. The samples were of good quality with a mosaic width of $\sim 0.05°$, $\sim 0.059°$, and $\sim 0.02°$ for the $x=0.33$, $x=0.30$, and $x=0.275$ samples, respectively. The x-ray scattering experiments were carried out on the XMaS CRG beam line BM28 (Ref. 14) at the ESRF, Grenoble, France. Measurements were carried out at a wavelength of 1 Å, which is close to the peak flux of the beam line and to increase the wave vector resolution a Ge(111) analyzer was used.

III. RESULTS

A. $x=0.33$

The sample was cooled to a base temperature of 10 K and a search was carried out for charge order satellites. These were located at modulations of (0.67,0,1) around the Bragg peaks with the strongest reflections occurring around the (4,0,4) Bragg reflection. This wave vector corresponds to a

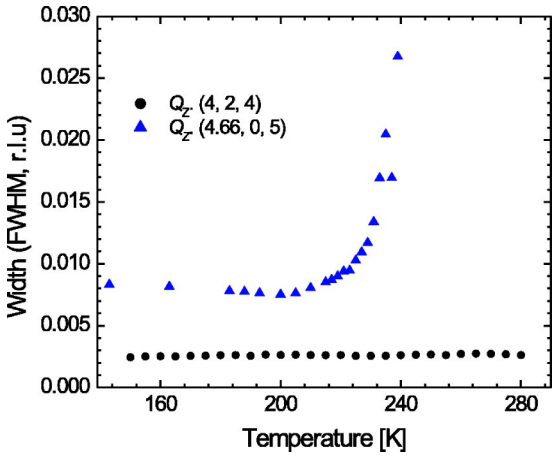

FIG. 3. (Color online) Temperature dependence of the width in Q_Z of the (4,2,4) Bragg peak and the (4.66,0,5) charge order peak as a function of temperature.

commensurability value of $\varepsilon = 0.337$, which is virtually commensurate with the lattice, i.e., a charge stripe occurs every three unit cells. A comparison with the Bragg reflections showed the charge stripe satellites to be substantially broader than the structural peaks, indicating that the charge stripes are far less correlated than the lattice.

Figure 3 shows the width of the (4,2,4) Bragg peak and the (4.66,0,5) charge order reflection as a function of temperature in the Q_Z direction where Q_Z is the reciprocal space direction normal to the scattering vector. The Bragg peak clearly shows no variation in width as a function of temperature, indicating that the structure shows no change in correlation. However, the width of the charge order changes as a function of temperature with a large broadening beginning at 200 K and continuing until it disappears at 240 K.

The (4.66,0,5) peak was the strongest charge order reflection and it was this that was measured. Scans were carried out in the three principle reciprocal space directions (*H*, *K*, and *L*) on the (4.66,0,5) charge order reflection. Figure 4 shows the fits to the experimental data. The charge order peak displayed a Gaussian line shape in the *H* direction and Lorentzian squared line shape in the *K* and *L* directions. The width of the charge order in the *H* and *K* directions was approximately equal, but the charge order peak was significantly broader in the *L* direction. The charge order was correlated over approximately 30 unit cells in the *H* and *K* directions but only 2 unit cells in the *L* direction—clearly demonstrating the two dimensional nature of the charge order. The temperature dependence of the integrated intensity, inverse correlation length, and commensurability of the (4.66,0,5) charge order reflection was measured as a function of temperature with scans being carried out in the *H*, *K*, and *L* directions at each temperature interval. The inverse correlation length ξ^{-1} was calculated using the equation

$$\xi_d^{-1} = \frac{2\pi}{d} w, \tag{1}$$

where *w* is the half width at half maximum of the reflection and *d* is the lattice constant parallel to the scattering vector.

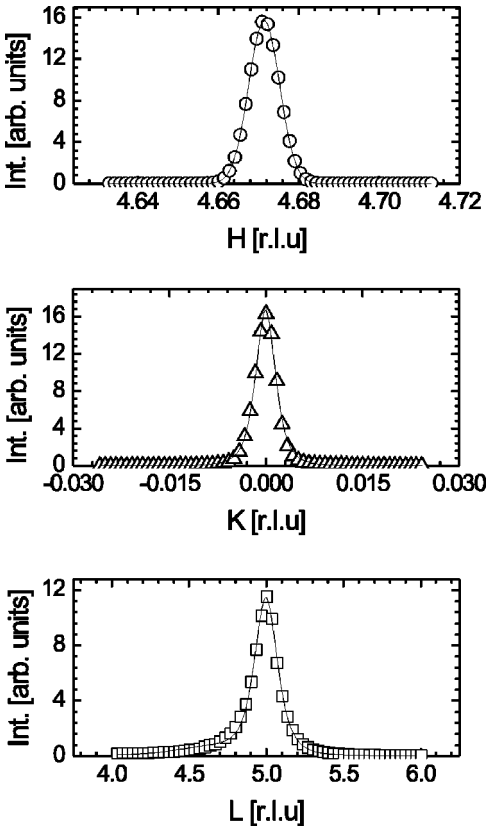

FIG. 4. Scans of the (4.66,0,5) charge ordering reflection along the *H*, *K*, and *L* directions. The solid lines show the fits with the *H* direction fitted to a Gaussian lineshape and the *K* and *L* directions displaying a Lorentzian squared line shape at 20 K.

The results for the integrated intensity, inverse correlation length, and commensurability are shown in Fig. 5. The intensity was normalized with the monitor to account for the decrease in the beam current with time. The intensity of the (4,0,4) Bragg peak was checked at regular temperature intervals to ensure there was no change in the intensity with temperature. The intensity of the Bragg peak showed no change with temperature and, hence, the behavior of the integrated intensity is valid and not due to experimental artifacts such as beam and sample movement. On heating from base temperature the integrated intensity was observed to gradually increase until 200 K. Upon further heating the intensity fell sharply and above 240 K only critical scattering fluctuations were observed. Earlier work on this sample by Du *et al.*[10] showed that the charge ordering transition was second order in nature and details of the charge ordering transition are dealt with in that paper. The transition temperature of 239 K is in agreement with the neutron measurements by Lee and Cheong[8] who calculated a charge ordering temperature of 240 K. However, there is a considerable difference in the behavior of the integrated intensity in our results and those reported in the neutron study. The neutron results showed a gradual decrease in intensity on heating from base temperature with an increase in the gradient occurring at the spin ordering temperature of 190 K. In the x-ray measurements we saw a gradual increase with a maximum in intensity at approximately 200 K before a sharp decrease occurs. This

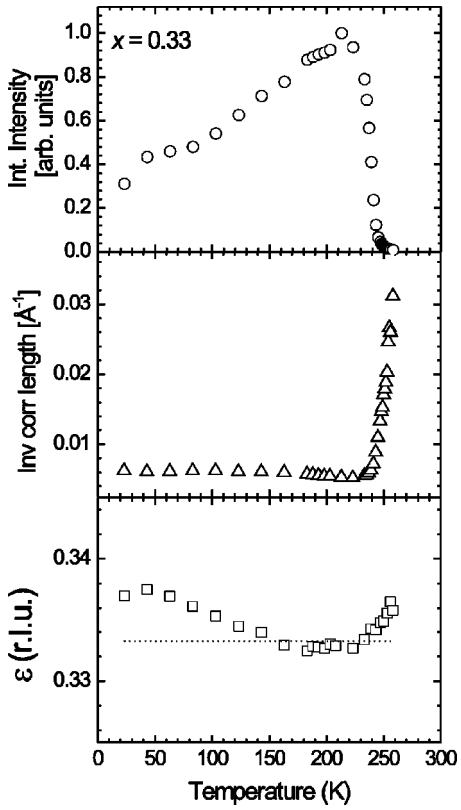

FIG. 5. Integrated intensity, inverse correlation length, and incommensurability of the (4.66,0,5) charge order peak in the H direction in the $x=1/3$ doped sample. The straight line in the bottom panel shows the $1/3$ position. Unless shown the error bars are smaller than the symbol size and were obtained from the errors on the fits at each temperature.

seems to indicate that there is an increase in the contrast between the charge stripes and, hence, an increase in the integrated intensity. The behavior of the integrated intensity will be discussed later in the paper in conjunction with the results for the 0.30 and 0.275 samples.

As the intensity increases it can be clearly seen that the wave vector is decreasing concurrently. The commensurability is not exactly equal to the $\varepsilon=1/3$ value shown by the straight line in the bottom panel of Fig. 5, and is slightly incommensurate with $\varepsilon=0.337$ at a base temperature of 20 K. As the temperature is increased it gradually moves towards $\varepsilon=1/3$, which is exactly commensurate with the lattice. This is consistent with the charge stripes gaining thermal energy, enabling them to move towards the commensurate position of $\varepsilon=1/3$. When the commensurability reaches this value it locks into $\varepsilon=1/3$, which is commensurate with the lattice and indicated on the graph by the dotted line. The inverse correlation length remained constant in the temperature range 10–160 K. However, at 160 K it began to decrease, indicating that the charge stripes were becoming more correlated. One possible reason for this behavior is that by locking into the commensurate value of $\varepsilon=1/3$ the charge order pattern is stabilized due to the coupling between the charge order and the lattice.

Above the magnetic ordering temperature of 190 K there is no further increase in intensity and it levels off and remains approximately constant until 220 K. At 220 K the integrated intensity begins to fall sharply and at the same temperature the inverse correlation length begins to increase along with a shift in the commensurability away from the commensurate $1/3$ value. The neutron studies in the lower doped samples have shown that the spin order stabilizes the charge order pattern and above T_N there is an increase in the inverse correlation length as the charge order becomes less stable. However, in the $x=0.33$ system the interaction between the charge order and the lattice the "commensurability effect" stabilizes the charge order pattern even in the absence of spin order as evidenced by a negligible change in the intensity and inverse correlation length between 190 and 220 K. At 220 K the holes have acquired enough thermal energy to break away from the charge stripes and the charge ordered state begins to melt. As mentioned in the earlier paper by Du *et al.*,[10] the charge ordering transition was determined to be 240 K with critical scattering fluctuations still existing above this temperature. The integrated intensity and inverse correlation length in the K and L directions behave in the same way as those properties in the H direction but they show no change in position beyond that due to thermal expansion. Throughout the charge ordered regime the charge ordering maintains its two-dimensional nature, with the L inverse correlation length being significantly larger than those in the H and K directions.

Finally, we discuss the behavior of the charge ordering close to the charge ordering temperature T_{CO}. The intensity of the charge order near T_{CO} includes a contribution from the critical scattering which is at a maximum at T_{CO}. Above 240 K only very weak charge scattering exists and this is caused by critical scattering due to dynamical spatial fluctuations in the charge stripe phase. In the earlier paper by Du *et al.*, this component was not subtracted and, hence, the intensity close to the transition temperature was overestimated. The critical scattering can be distinguished from the long range charge order by its different peak shape and width. The critical scattering component was subtracted and the resulting intensity profile was fitted to the power law equation:

$$(I) \propto \left(\frac{T_{CO}-T}{T_{CO}}\right)^{2\beta}. \tag{2}$$

The fitted parameters extracted from this fitting process on the intensity profile shown in Fig. 6 are $T_{CO}=239.0\pm0.2$ K and $2\beta=0.21\pm0.02$, which are similar to those obtained in the earlier results.

The measured exponent of 2β clearly demonstrates that below T_{CO} the charge stripes in the $1/3$ doped nickelate fall in the two dimensional class as tabulated in Collins[15] and this is reinforced by the measurements of the inverse correlation length. The calculated charge ordering temperature agrees with the previous neutron results and with the susceptibility and resistivity results. The critical scattering was observed up to 260 K. Throughout this range the measurements of the charge ordering showed that it retained its two-dimensional nature. The curve of the inverse correlation length between 240 and 260 K was fitted with a power law equation to determine the exponent ν of the inverse correlation length of the charge ordered satellite. The power law equation is

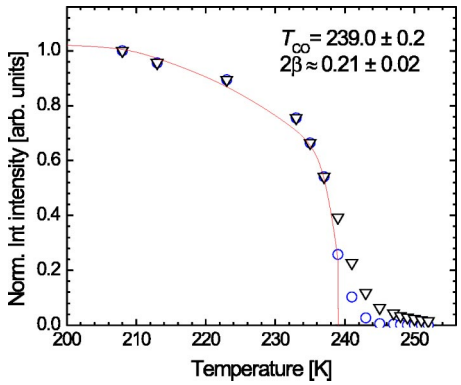

FIG. 6. (Color online) The temperature dependence of the integrated intensity of the (4.66,0,5) reflection near T_{CO}. The triangles show the total intensity, the circles the corrected intensity, and the line shows the power law fit.

$$\xi^{-1}(T) \propto \left(\frac{T - T_{CO}}{T_{CO}}\right)^{\nu}. \tag{3}$$

Fitting the data as in Fig. 7 gave the exponent as $\nu = 1.08 \pm 0.20$.

This is in excellent agreement with the predicted value of 1 expected for a two-dimensional system. The relatively large range of the critical scattering allowed the exponent to be determined accurately. The critical measurements of the inverse correlation length and intensity demonstrate that the charge stripes in the nickelate system show the behavior expected of a two-dimensional system.

To summarize, we found that the charge ordering within the 0.33 system to be intense and well correlated. The commensurability was initially 0.337 and on heating moved towards the commensurate position with it locking in at 160 K with an associated decrease in the inverse correlation length of the charge order pattern—"*the commensurability effect*." This is strong and stabilizes the charge stripe pattern even in the absence of the spin ordering above 190 K. The intensity decreases sharply above 220 K and above 240 K only critical scattering is present. Fitting the data near the charge ordering temperature showed the transition to be second order in nature.

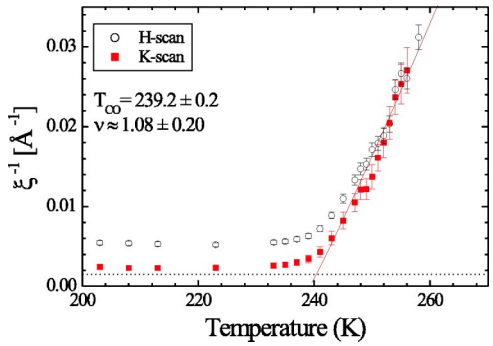

FIG. 7. (Color online) The temperature dependence of the inverse correlation length in the H and K directions of the (4.66,0,5) reflection near T_{CO}. The line shows the fit to the power law equation.

B. $x = 0.30$ and 0.275

Previously neutron scattering studies had been carried out on the $x = 0.275$ system by Lee *et al.*,[16] but no corresponding x-ray studies had been carried out to date. This study reports the first x-ray measurements carried out on these compositions.

The samples were cooled to a base temperature of 10 K in a displex cryostat and a search was carried out around the $(4,0,-4)$ Bragg peak in the $x = 0.30$ sample and around the (4,0,4) Bragg peak in the $x = 0.275$ sample. Superlattice reflections were located around the Bragg peaks consistent with the modulation wave vector $(2\varepsilon,0,1)$. At 10 K $\varepsilon = 0.317$ in the $x = 0.30$ sample and $\varepsilon = 0.295$ in the $x = 0.275$ doped sample. Superlattice reflections were measured as a function of temperature along the three principal directions in reciprocal space in triple axis geometry and data in all three directions was found to fit to a Lorentzian squared line shape. Scans were carried out on the (4,0,4) and $(4,0,-4)$ Bragg peaks in the H, K, and L directions. In all directions the superlattice peaks were significantly broader than the Bragg peaks.

The charge ordering satellite $(3.36,0,-3)$ was measured in the $x = 0.30$ sample and the (4.59,0,5) reflection in the $x = 0.275$ doped sample. The charge stripes in both samples were two dimensional in nature, as in the $x = 0.33$ sample, with the charge stripes well correlated in-plane, i.e., along the H and K directions and less well correlated along the L direction. It should be noted that the inverse correlation length in the L direction in the 0.33 sample was larger than that in the $x = 0.30$ and 0.275 systems. This is evidence that the charge order is more two dimensional in nature in the $x = 0.33$ system than in the $x = 0.275$ and $x = 0.30$ systems. (This result was not due to the instrumental resolution because a comparison revealed the instrumental resolution values of the 0.33, 0.30, and 0.275 samples to be virtually the same and to contribute a negligibly small width compared to the charge order reflections.)

Table I shows the inverse correlation length of the charge stripes in the $x = 0.33$, $x = 0.30$, and $x = 0.275$ doped samples and as a comparison the results for the (4,0,4) Bragg peak are tabulated. The charge ordering in the 0.30 and 0.275 systems was not as two dimensional in nature as in the 0.33 doped sample. In the H and K directions in both samples the charge order was correlated over approximately 25 unit cells,

TABLE I. Inverse correlation lengths for the charge order in the $x = 0.33$, $x = 0.30$, and $x = 0.275$ samples at 20 K as a comparison to the inverse correlation length of the (4,0,4) Bragg peak in the 0.275 sample is shown.

	Inverse correlation length (10^{-3} Å^{-1})		
Sample	H	K	L
$x = 0.33$	6.10 ± 0.07	2.66 ± 0.03	54.2 ± 0.4
$x = 0.30$	7.56 ± 0.08	4.60 ± 0.09	18.8 ± 0.4
$x = 0.275$	8.01 ± 0.14	4.89 ± 0.03	24.7 ± 0.3
Bragg	1.89 ± 0.04	1.39 ± 0.02	4.00 ± 0.10

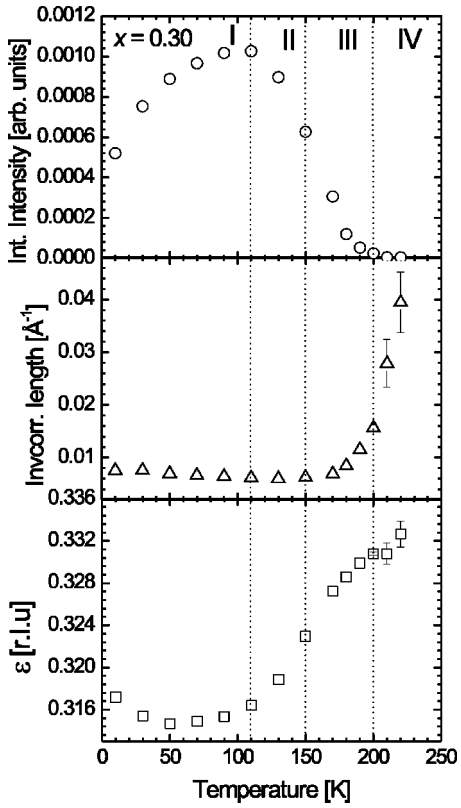

FIG. 8. Integrated intensity, inverse correlation length, and incommensurability of the $(3.36,0,-5)$ charge order peak in the H direction in the $x=0.30$ sample. Unless shown the error bars are smaller than the symbol size.

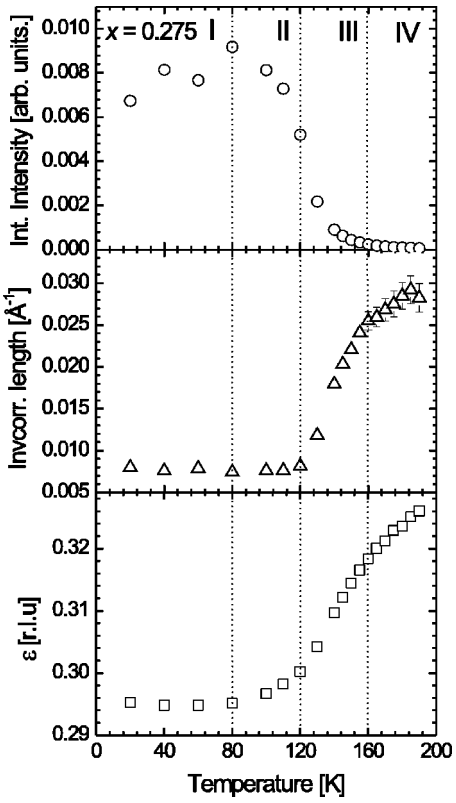

FIG. 9. Integrated intensity, inverse correlation length, and incommensurability of the (4.59,0,5) charge order peak in the H direction in the $x=0.275$ sample. Unless shown the error bars are smaller than the symbol size.

whereas in the L direction it was only correlated over approximately 5 unit cells. From these values we conclude the charge order is clearly two dimensional in nature but to a lesser degree than in the 0.33 sample.

The temperature dependence of the integrated intensity, inverse correlation length, and incommensurability for the $(3.36,0,-3)$ reflection along the H direction is shown in Fig. 8. There is a clear contrast with the behavior of the $x=0.33$ composition and there are in fact four clear regions for the charge stripe ordering. At low temperatures, between 10 K and 110 K, the charge reflections are intense and well correlated with a small inverse correlation length. The incommensurability was obtained by measuring the change in position of the superlattice peak in the H direction and in region I it is relatively constant with $\varepsilon=0.316$. In region II between 110 K and 150 K the integrated intensity begins to decrease and the incommensurability begins to increase towards the commensurate $\varepsilon=0.33$ value, and this is consistent with previous results[17] for the $x=0.289$ doped system. There is a slight decrease in the inverse correlation length in this region, indicating that the charge ordering is becoming more correlated. In region III between 150 K and 200 K the inverse correlation length increases, indicating that the charge stripes are becoming less correlated. The integrated intensity of the charge stripes continues to decrease and the incommensurability continues to increase towards the commensurate value $\varepsilon=1/3$. There is still weak scattering present above 200 K in regime IV, and this is attributed to critical scattering and the charge ordering here is weak and poorly correlated. The behavior of the integrated intensity and inverse correlation in the K and L directions is the same as in H but there is no change in the position beyond that due to thermal expansion.

The temperature dependence of the integrated intensity, inverse correlation length, and incommensurability of the (4.59,0,5) charge order reflection in the $x=0.275$ sample is shown in Fig. 9. Just as for the $x=0.30$ doped sample there are four clear regions. The charge ordering temperature is lower in the $x=0.275$ system with the integrated intensity beginning to decrease above 80 K and only critical scattering observed above 160 K. The incommensurability shows similar behavior to the $x=0.3$ sample, but due to the lower hole concentration the initial incommensurability at low temperatures is $\varepsilon=0.296$.

We shall now discuss the behavior of the charge ordering and we refer to the $x=0.30$ sample. In region I at base temperature the stripes are intense, have a small inverse correlation length and are incommensurate with $\varepsilon=0.316$. As the temperature is increased there is an increase in the charge density contrast and, hence, the integrated intensity increases. The behavior in region I is very similar to that of the 0.33 doped system with an increase in the integrated intensity but the effect is not as dramatic. Possible reasons for this behavior will be discussed in the next section. As the temperature is increased in region II the charge stripes gain more thermal energy and this enables them to overcome the Cou-

lomb repulsion and move towards the favored $\varepsilon=1/3$ value and thus the incommensurability wave vector increases. This change in position was significantly larger than in the 0.33 system. There is a decrease in the integrated intensity as the temperature is increased into region II. As the temperature is increased the holes gain thermal energy, allowing them to overcome the interactions with the lattice which fix them on the charge stripe. This lowers the hole concentration on the charge stripes and as a result the integrated intensity decreases. To minimize the Coulomb repulsion the charge stripes straighten, causing the inverse correlation length to decrease slightly, indicating an increase in the degree of stripe correlation. The boundary of regions II and III corresponds to the spin ordering temperature T_N. The charge stripes are no longer stabilized by the spin stripes and coupled with the increased thermal energy begin to vibrate; due to this there is a sharp increase in the inverse correlation length. In region III there is a continuation of the decrease in integrated intensity and increase in the incommensurability as the holes continue to gain thermal energy. In region IV only critical scattering exists and this is very weak and virtually uncorrelated. The wave vector is close to the commensurate value but the charge ordering disappears before ε reaches the stable $1/3$ value. In the lower doped $x=0.275$ sample the charge stripes are less stable and initially further apart resulting in lower Coulomb repulsion. Therefore, less thermal energy is required to overcome the Coulomb repulsion, and hence move the stripes towards the stable configuration. For this reason the charge ordering enters region II at 80 K as opposed to 110 K in the $x=0.30$ doped sample. The broadening of the inverse correlation length corresponds to the magnetic ordering temperature observed by Lee and Cheong[8] in the aforementioned study of the $x=0.275$ composition. The neutron results for the 0.275 composition revealed no initial increase in integrated intensity; instead it remains constant at low temperatures. The charge ordering then behaves in a similar way to the $x=0.30$ doped sample, but due to the lower doping level the spin and charge ordering temperatures are lower. This is in agreement with that seen in previous studies with the charge and spin ordering temperatures decreasing from $x=0.33$.

IV. DISCUSSION

In all three samples there is an initial increase in the integrated intensity as the temperature is increased. This effect is most significant in the $x=0.33$ doped system but it is also observed in the 0.30 and 0.275 systems. In each sample measurements of the Bragg peak intensity confirmed that it was not as a result of sample or beam movement. Our measurements of the integrated intensity showed a considerable difference when compared with the neutron scattering results. In the neutron scattering study of the 0.33 by Cheong *et al.*[7] and the study on 0.33 and 0.275 by Lee *et al.*[16] the integrated intensity demonstrated a gradual decrease with temperature. This is in clear contrast to our results where an inital increase in intensity is seen. We can offer no definite explanation for the discrepancy between the neutron and x-ray techniques. Both techniques are sensitive to long-range correlations in the electron density and reflect distortions in the electron density. Both would be expected to show similar results with respect to the integrated intensity. There has been some discussion as to whether a movement of holes from the nickels (site centered stripes) to the oxygens (bond centered stripes) could be responsible. However, Tranquada *et al.*[18] in a study of $La_2NiO_{4+\delta}$ for $\delta=0.133$ determined that the movement of the holes from the Ni sites to the oxygens only became significant above the magnetic ordering temperature. This does not explain the low temperature behavior which occurs well below the magnetic ordering temperature. Further study is required to clarify the discrepancy between the x-ray and neutron measurements.

A possible explanation for the behavior of the integrated intensity is the influence of the spin exchange interactions. At low temperatures the effect of the exchange interactions is strong, and this favors a uniform charge distribution across the charge stripe. This lowers the magnitude of the associated lattice modulation and, hence, the charge density difference between the hole rich and hole poor regions. The spin exchange interactions compete with the effects of Coulombic repulsion which seeks to maximize the distance between the charge. As the temperature is increased the holes gain more thermal energy and overcome the spin exchange interactions, and to minimize Coulombic repulsion the holes attempt to maximize the distance between them. This increases the magnitude of the lattice modulation in the hole rich areas and, hence, the contrast in the charge density between the hole rich and hole poor regions and the intensity increases. In the $x=0.33$ sample this continues until the intensity maximizes at the spin ordering temperature of 190 K. In the $x=0.30$ and 0.275 samples this effect is also observed but possibly because the charge order is less stable the intensity begins to decrease before reaching the magnetic ordering temperature. This is only a proposed model, but a recent experiment by Schußler-Langeheine *et al.*[19] has reported the observance of a resonance in the scattered intensity for the charge order in $La_{1.8}Sr_{0.2}NiO_4$ when the energy was tuned to the Ni L_{II} and L_{III} edges. This confirmed the Ni^{2+}/Ni^{3+} charge order pattern and further experiments at the L edges may test the validity of the proposed model.

When comparing the behavior of the incommensurability between the three doping levels we refer the reader to Fig. 10, which shows the temperature dependence of the incommensurability. In all samples the charge order attempts to move towards the commensurate $\varepsilon=1/3$ value. In the $x=0.33$ system there is a small change in the incommensurability as it moves towards the $\varepsilon=1/3$ value. Once this position is reached there is a stabilization of the charge order. In the lower doped samples the incommensurability also tends towards the stable $\varepsilon=0.33$ value but the charge ordering in both samples disappears before reaching the stable position. Table I summarizes the inverse correlation lengths measured in region I for the $x=0.33$, $x=0.30$, and $x=0.275$ samples. In all samples the charge ordering is two dimensional in nature and is significantly less correlated than the crystal lattice. As the doping is decreased from the stable configuration of $x=0.33$, the inplane inverse correlation lengths increase, indicating that the charge ordering is becoming more disordered. In the $x=0.33$ doped sample the charge and spin ordering coincide at the same position and as result the charge order-

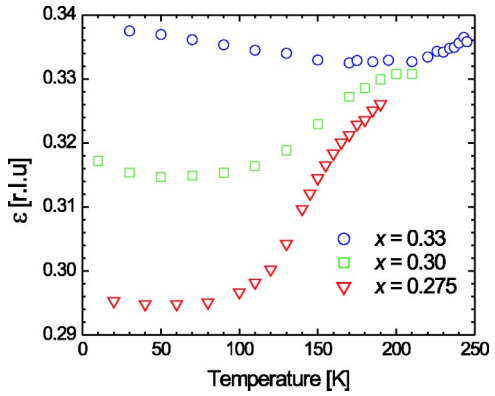

FIG. 10. (Color online) The temperature dependence of the commensurability, ε, in the $x=0.33$, $x=0.30$, and $x=0.275$ samples.

ing is stabilized. The data from the 0.33 system showed that the commensurability effect from the coupling between the lattice and the charge order also stabilized the charge order even in the absence of spin order. As the doping in the system is decreased the charge and spin stripes no longer occur at the same position and this results in the charge stripes becoming more disordered within the plane as the doping level moves away from $x=0.33$. The charge order is more two dimensional in nature in the 0.33 sample than in the 0.30 and 0.275 doped samples and we do not know why this is the case.

In the 0.33 doped composition the integrated intensity continued to increase until the magnetic ordering temperature. In the $x=0.30$ and 0.275 systems the intensity begins to decrease before the spin ordering temperature because the charge stripes are not as stable as in the 0.33 system. In the 0.33 system the charge stripes are stabilized when they reach the commensurate value and this effect stabilizes the charge order pattern even above the magnetic ordering temperature. However, in the $x=0.30$ and $x=0.275$ systems the charge ordering is incommensurate and not stabilized by interactions between the charge order and the lattice. Above the magnetic ordering temperature the inverse correlation length in the 0.30 and 0.275 systems begins to increase sharply because in these systems long-range charge order cannot exist in the absence of magnetic order.

V. CONCLUSIONS

By using high resolution x-ray scattering we have confirmed that the charge stripes become more disordered as the doping is reduced from the commensurate $x=0.33$ value. These results show that the charge stripes in the $x=0.30$ and $x=0.275$ samples are still highly correlated but less correlated in-plane than for $x=0.33$. However, the charge stripes are less two dimensional in the lower doped samples evidenced by a smaller inverse correlation length in along the L direction. In the $x=0.33$ composition the charge order was slightly incommensurate at low temperatures and gradually moved towards and then "locked in" to the commensurate position of 0.333. This was accompanied by a stabilization of the charge order. In the $x=0.30$ and 0.275 systems the charge order was far from the commensurate position. However, as the temperature was increased the commensurability also tended towards the stable $\varepsilon=0.33$ value when the stripes gain enough thermal energy to overcome Coulomb repulsion. However, the charge order disappeared in both samples before it could reach the stable position.

The inverse correlation length shows different behavior between the $x=0.33$ composition and the lower doped compositions. In the 0.30 and 0.275 systems the inverse correlation length increases sharply at the spin ordering temperature, evidence that the spin order stabilizes the charge order pattern. However, in the 0.33 doped system the spin ordering temperature is 190 K but the charge order shows no change in correlation until 220 K—well above T_N. This suggests that the interaction between the charge order and the lattice stabilizes the charge order pattern in the 0.33 system, i.e., a commensurability effect.

In the low temperature phase an increase in the charge ordering intensity is observed and on heating in all samples. This effect was most significant in the 0.33 system where the intensity increased until T_N was reached. This increase in intensity was not observed in any of the previous neutron studies and we can offer no definite explanation for this and it clearly requires further study.

Further studies will be reported on other compositions in the $La_{2-x}Sr_xNiO_4$ system to allow a fuller understanding of the charge ordering for all nickelate doping levels.

ACKNOWLEDGMENTS

This work is supported by a grant from the Engineering and Physical sciences Research Council. The authors would like to thank the XMaS beam line team of D. F. Paul, S. Brown and P. Thompson for their valuable help, to S. Beaufoy and J. Kervin for additional support and EPSRC for financial support. P.D.S. and S.B.W. would like to thank EPSRC for additional support. P.D.H. thanks the University of Durham for support through the Sir James Knott Foundation.

*Electronic address: p.d.hatton@durham.ac.uk

[1] J. M. Tranquada, B. J. Sternlieb, J. D. Axe, Y. Nakamura, and S. Uchida, Nature (London) **375**, 561 (1995).

[2] R. J. Cava, B. Batlogg, T. T. Palstra, J. J. Krajewski, W. F. Peck, A. P. Ramirez, and L. W. Rupp, Phys. Rev. B **43**, 1229 (1991).

[3] V. Sachan, D. J. Buttrey, J. M. Tranquada, J. E. Lorenzo, and G. Shirane, Phys. Rev. B **51**, 12742 (1995).

[4] H. Yoshizawa, T. Kakeshita, R. Kajimoto, T. Tanabe, T. Katsufuji, and T. Tokura, Physica B **241**, 880 (1998).

[5] J. M. Tranquada, D. J. Buttrey, and V. Sachan, Phys. Rev. B **54**, 12318 (1996).

[6] A. Vigliante, M. von Zimmermann, J. R. Schneider, T. Frello, N.

H. Andersen, J. Madsen, D. J. Buttrey, D. Gibbs, and J. M. Tranquada, Phys. Rev. B **56**, 8248 (1997).
[7] S. W. Cheong, H. Y. Hwang, C. H. Chen, B. Batlogg, L. W. Rupp, and S. A. Carter, Phys. Rev. B **49**, 7088 (1994).
[8] S. H. Lee and S. W. Cheong, Phys. Rev. Lett. **79**, 2514 (1997).
[9] H. Yoshizawa, T. Kakeshita, R. Kajimoto, T. Tanabe, T. Katsufuji, and Y. Tokura, Phys. Rev. B **61**, R854 (2000).
[10] C.-H. Du, M. E. Ghazi, Y. Su, I. Pape, P. D. Hatton, S. D. Brown, W. G. Stirling, M. J. Cooper, and S.-W. Cheong, Phys. Rev. Lett. **84**, 3911 (2000).
[11] P. D. Hatton, M. E. Ghazi, S. Brown, and S. W. Cheong, Int. J. Mod. Phys. B **14**, 3488 (2000).
[12] M. E. Ghazi, C. H. Du, P. D. Hatton, S. Brown, and S. W. Cheong, in *Proceedings of 1st Regional Conference on Magnetic and Superconducting Materials* (MSM-99), Vol. 1, p. 275 (2000).
[13] D. Prabhakaran, P. Isla, and A. Boothroyd, J. Cryst. Growth **237**, 815 (2002).
[14] S. D. Brown, L. Bouchenoire, D. Bowyer, J. Kervin, D. Laundy, and M. J. Longfield, J. Synchrotron Radiat. **8**, 1172 (2001).
[15] M. F. Collins, *Magnetic Critical Scattering* (Oxford University Press, New York, 1989).
[16] S.-H. Lee, S.-W. Cheong, K. Yamada, and C. F. Majkrzak, Phys. Rev. B **63**, 060405 (2001).
[17] R. Kajimoto, T. Kakeshita, H. Yoshizawa, T. Tanabe, T. Katsufuji, and Y. Tokura, Phys. Rev. B **64**, 144432 (2001).
[18] J. M. Tranquada, P. Wochner, A. R. Moodenbaugh, and D. J. Buttrey, Phys. Rev. B **55**, R6113 (1997).
[19] C. Schußler-Langeheine, J. Schlappa, Z. Hu, M. W. Haverkort, M. Benomar, O. Friedt, E. Schierle, H. Ott, E. Weschke, G. Kaindl *et al.*, Verh. Dtsch. Phys. Ges. **2**, 432 (2004).